OUKA
The University of Osaka
Institutional Knowledge Archive

Title	Orofacial Proprioceptive Thalamus in the Rat
Author(s)	Ali, Md Sams Sazzad
Citation	大阪大学, 2019, 博士論文
Version Type	VoR
URL	https://doi.org/10.18910/72243
rights	
Note	

The University of Osaka Institutional Knowledge Archive : OUKA

https://ir.library.osaka-u.ac.jp/

The University of Osaka

Orofacial Proprioceptive Thalamus in the Rat

Ph.D. Thesis

Md Sams Sazzad Ali

Osaka University Graduate School of Dentistry

2019

ABSTRACT

The ascending pathway mediating proprioception from the orofacial region is still not fully known. The present study elucidated the relay of jaw-closing muscle spindle (JCMS) inputs from brainstem to thalamus in rats. We injected an anterograde tracer into the electrophysiologically identified supratrigeminal nucleus (Su5), known to receive JCMS input. Many thalamic axon terminals were labeled and were found mainly contralaterally in a small, unpredicted area of the caudo-ventromedial edge (VPMcvm) of ventral posteromedial thalamic nucleus (VPM). Electrical stimulation of the masseter nerve and passive jaw movements induced large responses in the VPMcvm. The VPMcvm is far from the rostrodorsal part of ventral posterolateral thalamic nucleus (VPL) where proprioceptive inputs from the body are represented. After injection of a retrograde tracer into the electrophysiologically identified VPMcvm, many neurons were labeled almost exclusively in the contralateral Su5, whereas no labeled neurons were found in the principal sensory trigeminal nucleus (Pr5) and spinal trigeminal nucleus (Sp5). In contrast, after injection of a retrograde tracer into the core of VPM, many neurons were labeled contralaterally in the Pr5 and Sp5, but none in the Su5. We conclude that JCMS input excites trigeminothalamic projection neurons in the Su5 which project primarily to the VPMcvm in marked contrast to the other proprioceptors and sensory receptors in the orofacial region which project to the core VPM. These

findings suggest that lesions or deep brain stimulation (DBS) in the human equivalent of VPMcvm may be useful for treatment of movement disorders (e.g., Orofacial tremor) without affecting other sensations.

Keywords: orofacial deep sensation, VPM, trigeminal, supratrigeminal nucleus, thalamotomy, DBS

Abbreviations

3V	third ventricle
7n	facial nerve
10	dorsal motor nucleus of vagus
12	hypoglossal nucleus
ABC	avidin-biotin-peroxidase complex
APT	anterior pretectal nucleus
AVM	area ventral to the Mo5 and medial to the Pr5
BDA	biotinylated dextranamine
CL	centrolateral thalamic nucleus
CM	central medial thalamic nucleus
Contra	contralateral
Cu	cuneate nucleus
DAB	diaminobenzidine
DBS	deep brain stimulation
FG	fluorogold
Fr	faciculus retroflexus
Gr	gracile nucleus
HRP	horseradish peroxidase
I5	intertrigeminal region

IMD	intermediodorsal thalamic nucleus
Ipsi	ipsilateral
JCMS	jaw-closing muscle spindle
KF	Kölliker-Fuse nucleus
LHb	lateral habenular nucleus
LPB	lateral parabrachial nucleus
m5	trigeminal motor nerve
Me5	mesencephalic trigeminal nucleus
me5	mesencephalic trigeminal tract
MD	mediodorsal thalamic nucleus
MHb	medial habenular nucleus
ml	medial laminiscus
Mo5	trigeminal motor nucleus
MPB	medial parabrachial nucleus
PB	parabrachial nucleus
PC	paracentral thalamic nucleus
PF	prafascicular thalamic nucleus
PhB	phosphate buffer
PhBS	phosphate buffered saline
Po	posterior thalamic nucleus
Pr5	principal sensory trigeminal nucleus
PV	paraventricular thalamic nucleus

scp	superior cerebellar peduncle
SO	superior olive
Sol	nucleus of the solitary tract
Sp5	spinal trigeminal nucleus
sp5	spinal trigeminal tract
Sp5C	Sp5, caudal part
Sp5I	Sp5, interpolar part
Sp5O	Sp5, oral part
Su5	supratrigeminal nucleus
TMB	tetramethyl benzidine
Vim	ventral intermediate thalamic nucleus
VM	ventromedial thalamic nucleus
VPL	ventral posterolateral thalamic nucleus
VPLo	oral part of the VPL
VPM	ventral posteromedial thalamic nucleus
VPMcvm	caudo-ventromedial edge of the VPM
VPPC	parvicellular part of ventral posterior thalamic nucleus
WGA-HRP	wheat-germ agglutinin conjugated horseradish peroxidase

Introduction

Proprioceptive sensation from the body is conveyed to the rostrodorsal shell (oral) region (or VPLo) of the ventral posterolateral thalamic nucleus (VPL) (monkey, Friedman and Jones 1981; Maendly et al. 1981; Jones and Friedman 1982; Jones et al. 1982; cat, Andersson et al. 1966; rat, Francis et al. 2008). However, little is known about the thalamic relay of proprioceptive inputs from the orofacial area. Thus, the major aim of this study is to obtain detailed information on the rat thalamic relay of orofacial proprioceptive information. Jones and Friedman (1982) predicted that the relay site for orofacial proprioception is located in the rostrodorsal part of the ventral posteromedial thalamic nucleus (VPM) (medially adjacent to the VPLo), but direct evidence is still lacking. Although the cutaneous sensation and deep sensation (including proprioception) arising in the body are conveyed by the primary afferents arising from the dorsal root ganglion neurons, the orofacial sensations are conveyed by the primary afferents arising not only from the trigeminal ganglion neurons (comparable to the dorsal root ganglion neurons) but also from the trigeminal mesencephalic nucleus (Me5) neurons (for review, see Dubner et al. 1978; Taylor 1990). Luo and Dessem (1995) and Luo et al. (1995) reported in rats the existence of neurons in the supratrigeminal nucleus (Su5) which receive proprioceptive inputs from the jaw-closing muscle spindles (JCMSs) and project to the contralateral VPM, but they did not provide the detailed projection termination sites in the VPM. In addition, earlier studies including those of Luo and colleagues cited above, were conducted without defining the exact location of the Su5. Furthermore the definition of Su5 in previous rat studies are inconsistent and even contradictory (e.g., rat brain atlas

by Swanson, 1992, and Paxinos and Watson, 1998, 2007, 2014). Therefore, Fujio et al. (2016) have recently determined the exact location of the rat Su5 according to the original definition of the Su5 by Lorente de Nó (1922, 1933): the true "Su5" is a premotoneuron pool in the trigeminal reflex arc. They have cytoarchitechtonically identified a restricted area in the supretrigeminal region which receives strong projections from Me5 neurons conveying inputs from the jaw-closing muscle spindles (JCMSs), and, thus, have defined this area as true "Su5". This study also revealed that the location of true "Su5" that does not correspond to the location of Su5 shown in the rat atlases by Paxinos and Watson (1998, 2007, 2014), but overlaps to some extent with the "trigeminal transition zone" which was newly introduced in the supratrigeminal region by Paxinos and Watson (2007, 2014). Therefore in the present study, we have applied the definition of the true "Su5" described by Fujio et al. (2016) to identify the thalamic "orofacial proprioception-center" receiving JCMS inputs. To this end, we examined the thalamic projections from the true "Su5" by using neuronal tract tracing and electrophysiological recording methods in rats.

Earlier electrophysiological studies demonstrated that cutaneous and proprioceptive sensations from the body are separately encoded in different regions of VPL (in the core (middle) region and rostrodorsal shell or rostral (oral) region of VPL) (human: Ohye et al. 1990, 1994; monkey: Friedman and Jones 1981; Maendly et al. 1981; Jones and Friedman 1982; Jones et al. 1982; cat: Andersson et al. 1966; rat: Francis et al. 2008). These studies also demonstrated that all kinds of proprioceptive sensations from the muscle spindle, fascia, tendon and joint capsule converge in the rostrodorsal shell or rostral (oral) region of VPL. In contrast, Luo and Dessem (1995) showed that the efferents from the Su5 which receive JCMS inputs conveyed by the Me5 neurons and

those from the principal sensory trigeminal nucleus (Pr5) and spinal trigeminal nucleus (Sp5) receiving the orofacial sensations (including non-Me5 deep sensory inputs) via the trigeminal ganglion neurons. Thus, the present study was designed to re-examine whether the JCMS proprioceptive sensations mediated via the Su5 neurons and the other orofacial sensations mediated via the Pr5 and Sp5 neurons are encoded convergently or separately in the VPM, by comparing thalamic terminal distributions of distinct populations of trigeminal neurons.

Determining the exact thalamic relay of orofacial proprioception may provide useful information for the neurosurgical treatment of some orofacial tremor and movement disorders in patients. Indeed, electrical lesions (thalamotomy) or deep brain stimulation (DBS) in the ventral intermediate thalamic nucleus (Vim), which corresponds to the VPLo in non-human primates and receives proprioceptive inputs from the body, is applied to improve motor systems in various movement-disorder patients (e.g. parkinsonian patients) (Narabayashi and Ohye 1980; Ohye et.al. 1989; Lenz et al. 1990, 1994; Ohye 2000; Hamani et al. 2006). There exist several orofacial movement disorders such as oromandibular dystonia, essential tremor and parkinsonian resting tremor in the jaw (Clark et al. 1993; Erer and Jankovic 2007; Wolraich et al. 2010; Karp and Alter 2016). However surgical target for these disorders remains unclear. The results of the present study showing the exact thalamic relay of orofacial proprioception in rats may provide useful insights for the treatment of some of these disorders.

Materials and methods

Animals

A total of 30 Wistar rats ranging in weight from 230 g to 330 g was used. All experimental procedures were approved by the Osaka University Graduate School of Dentistry Intramural Animal Care and Use Committee in accordance with the guidelines of NIH, USA. We made efforts to minimize the number of animals used.

Experimental procedures

In all animals used, sodium pentobarbital (55 mg/kg, Dainippon Sumitomo Pharma, Osaka, Japan) with supplementary doses of sodium pentobarbital (10 mg/kg) was intraperitoneally injected for anesthesia at such a level that neither corneal reflex nor spontaneous eye movement were apparent. In the first, second and third experiments, an incision was made in the buccal skin on the right side, in order to expose the masseter nerve (which innervates the JCMSs), and it was dissected free from the masseter muscle. In the fourth experiment, to expose the lingual nerve on the right side, after an incision was made in the submandibular skin, the mylohyoid muscle was torn, and the lingual nerve was the dissected free. To expose the infraorbital nerve distal to the infraorbital foramen, an incision was made in the infraorbital skin, and the nerve was dissected free. All incisions of the skin were performed under local anesthesia with lidocaine hydrochloride. For the electrical stimulation of these nerves (single pulse, 200 μsec duration, 1 Hz), silver hook bipolar stimulation electrodes were attached to the individual nerves. Subsequently, the animal's head was mounted in a stereotaxic apparatus. The rectal temperature was

maintained between 36°C and 38°C with a heating pad, and ECG was continuously monitored. The atlas of the rat brain by Paxinos and Watson (1998) was chiefly used for the delineation of brain structures and determination of coordinates for stereotaxic micropipette insertion.

In the first experiment, we injected an anterograde tracer, biotinylated dextran amine (BDA, 10,000 MW, Molecular Probes, Eugene, OR, USA), into the Su5. First, the right parietal bone was partly removed with the aid of a dental drill. Then, a small part of dura was cut to insert a glass micropipette filled with 4% BDA dissolved in saline, obliquely with an 18° rostral-to-caudal inclination into the rostrolateral pons. According to the criteria reported in a previous study (Fujio et al. 2016), the Su5 was identified by recording the field potentials in response to electrical stimulation of the masseter nerve and by unit recordings of responses to passive, sustained jaw-opening movements. For jaw opening movements (muscle stretch), the mandible was manually depressed with a hand-held plastic probe inserted into the mouth. Signals recorded from the microelectrode were amplified, filtered (300 Hz to 3 kHz), and stored in a computer at the sampling rate of 20 kHz (field potentials) or 10 kHz (unit activity). Subsequently, BDA was injected iontophoretically with 2.0 μA positive pulses (300 msec, 2 Hz) for 7-10 minutes into the identified Su5. After the tracer injection, stimulation electrodes were detached from the masseter nerve, and all wounds were sutured. Then, an antibiotic (cefotiam hydrochloride, 66mg/kg, Takeda Pharmaceutical Company, Osaka, Japan) and an analgesic (flurbiprofen axetil, 3.3 mg/kg, Kaken Pharmaceutical, Tokyo, Japan) were given i.p., and the animals were allowed to recover from the anesthesia in their cages. During the postinjection survival, the animals were monitored on a daily basis to assess

body weight, general behaviors, and any postoperative complications such as bleeding or inflammation.

In the second experiment, we used local field potential and unit recordings to identify the region of VPM and surrounding thalamus which received sensory inputs from JCMSs elicited by electrical stimulation of the masseter nerve and passive, sustained jaw-opening movements. Before the animals were fixed to stereotaxic apparatus, an incision was made in the anterior neck skin, the sternothyroid muscle was torn, and the trachea was cannulated. Then, a small bur hole was made on the parietal part of the skull on the left side to expose the dura. A small part of the dura was cut to vertically insert a glass microelectrode, filled with 2.0 M potassium citrate, into the brain. The evoked field potentials were mapped in and around the caudo-ventromedial part in the VPM (4.16 mm caudal to bregma, 2.10 mm lateral, and 3.30 mm dorsal to the interaural line) where the densest BDA-labeled terminals were found in a representative case, R317, in the first experiment as shown in Fig. 3A-C. For the mapping of field potentials, the microelectrode was driven down in 25 μm steps and the distance between successive recording tracks was 100 μm. During the electrophysiological mapping, the animals were immobilized with a neuromuscular junction blocker, vecuronium bromide (0.02 mg/kg, i.v., Sankyo Co.Tokyo, Japan), and artificially ventilated. To keep the animal immobilized, vecuronium bromide was added (0.02 mg/kg, i.v.) several times throughout the experiment. After the mapping, the electrode was changed to the one filled with 3% horseradish peroxidase (HRP, Toyobo, Osaka, Japan) dissolved in saline for the confirmation of recording sites (but not for the tracing study). The HRP injection was

iontophoretically performed by delivering 2.0 μA positive pulses (300 msec, 2 Hz) for 20 seconds.

In the third and fourth experiments, a retrograde tracer, wheat-germ agglutinin conjugated horseradish peroxidase (WGA-HRP, Sigma Chemical Co., St. Louis, MO) or Fluorogold (FG, Fluorochrome, Englewood, CO, USA) was injected into distinct regions of the VPM. In these experiments, the cannulation of the trachea and artificial ventilation was not performed. A glass microelectrode filled with 3% WGA-HRP dissolve in 0.05 M Tris buffer or with 1% FG in 0.1 M sodium acetate buffer was inserted into the VPM. In the third experiment, WGA-HRP or FG was iontophoretically injected by delivering 2.0 μA positive pulses (300 msec, 2 Hz) for 7-12 minutes for WGA-HRP or for 10-15 minutes for FG into the region of VPM where the largest field potentials were recorded during the electrical stimulation of the masseter nerve and during passive, sustained jaw-opening movements. In the fourth experiment, WGA-HRP or FG was injected into the VPM where the largest field potentials were recorded during the electrical stimulation of the lingual nerve or infraorbital nerve. After the tracer injections in the third and fourth experiments, the animals were treated in the same way as the above-mentioned animals receiving the BDA injection into the Su5.

Histology

After a postinjection survival of 6-8 days in BDA or FG injection cases, or 2-3 days in WGA-HRP injection cases, or soon after HRP injection cases, the animals were re-anesthetized deeply with an i.p. injection of sodium pentobarbital (100 mg/kg) and perfused through the ascending aorta with 100 ml of 0.02 M phosphate-buffered saline (PhBS, pH 7.4) followed by 300 ml of fixative. A fixative containing 1.0%

paraformaldehyde and 1.0% glutaraldehyde in 0.1 M phosphate buffer (PhB) (pH 7.4) was used for WGA-HRP injection cases, and one containing 4% paraformaldehyde in 0.1 M PhB (pH 7.4) was used for the other cases. Then, the entire brain was removed and placed in 25% sucrose in 0.02 M PhB at 4^{o}C for a few days. It was cut coronally (60-μm thickness) on a freezing microtome. The serial sections were alternately divided into three sets.

For the detection of BDA, all sets of alternate serial sections were washed in 0.02 M PhBS (pH 7.4) and preincubated in 0.02 M PhBS containing 0.01% H_2O_2 and 0.75% Triton X-100, as described previously (Sato et al., 2013; Akhter et al., 2014). The sections were then incubated in 0.02 M PhBS containing avidin-biotin-peroxidase complex (ABC) diluted at 1:100. The sections were reacted in diaminobenzidine (DAB) solution (0.1 M PhB [pH 7.4] containing 0.04% DAB, 0.006% H_2O_2 and 0.08% nickel ammonium sulphate). For the detection of HRP injection sites, all sets of alternate serial sections were reacted in a DAB solution. For the detection of WGA-HRP, two sets of alternate serial sections were processed according to the tetramethyl benzidine (TMB) method (Mesulam 1978). The remaining set of sections was reacted in a DAB solution. In FG injection cases, one set of alternate serial section was not reacted. For the detection of FG, the remaining two sets of the sections were incubated in 0.02 M PhBS containing 3% normal goat serum, 0.2% Triton X-100 and polyclonal rabbit anti-FG primary antibody (Chemicon, CA, USA: product No. AB153) diluted at 1:10,000. The sections were then incubated in 0.02 M PhBS containing biotinylated goat anti-rabbit immunoglobulin G (Vector) diluted at 1:400, and in 0.02 M PhBS containing ABC diluted at 1:100. Subsequently, the sections were incubated in a DAB solution. In the control experiments

where the FG injection was not made or the anti-FG primary antibody was omitted, no labeling was detected.

Finally, all sets of sections in all experiments were mounted on gelatin-coated slides, and dried. One set of sections in BDA injection cases, two sets of sections in HRP injection cases, one set of DAB-reacted sections in WGA-HRP injection cases, and one set of above-reacted sections in FG injection cases were counterstained with Thionin or Neutral Red. Then, all sections in all experiments, except for sections reacted with TMB, were dehydrated in graded alcohol, cleared in xylene, and coverslipped. Sections reacted with TMB were cleared directly with xylene without dehydration in alcohol.

Data analysis

The field potentials recorded in all of the above experiments were stored on a personal computer, and offline analysis was performed with computer assistance (PowerLab 8/30, ADInstruments, Sydney, Australia). Responses to seven to ten successive stimuli were averaged at each recording site.

We drew the brain structures, tracer injection sites, retrogradely labeled neuronal cell bodies, anterogradely labeled axonal fibers and terminals, and electrode penetration tracks by use of a camera lucida attached to the light microscope. The extent of the FG injection site was judged by observing the sections under an epifluorescence microscope with filters providing ultraviolet excitation light, as described previously (Yoshida et al.1991, 2009). The extent of the WGA-HRP injection site was judged by observing the sections reacted with DAB, as described previously (Yoshida et al. 1991, 1992). The number of retrogradely labeled neurons was counted in every third section.

Photomicrographs of selected sections were taken by a digital camera (Pixera Pro 150ES, CA, USA) connected to the light microscope. Photomicrographs of retrogradely WGA-HRP-labeled neuronal cell bodies were taken under the dark field illumination with poloarizing filters. All photomicrographs were processed using Photoshop CS2 (Adobe Systems, CA, USA) with a slight adjustment of the image's contrast.

Results

Anterograde labeling of thalamic projections from Su5 neurons

In the first experiment, we examined the thalamic projection patterns of Su5 neurons that receive proprioceptive inputs from JCMS receptors. The electrophysiological identification of the Su5 was described elsewhere (Fujio at al. 2016). Briefly, we targeted the brain stem region (assumed to be Su5) where we could record a small negative field potential (with around 1 msec latency) in response to electrical stimulation of the masseter nerve (innervating JCMS receptors; e.g., Fig. 1A) and /or neurons that increased their firing during passive, sustained jaw-opening movements (e.g., Fig 1B). Subsequently we injected an anterograde tracer, BDA, into this electrophysiologically identified site in Su5. The locations of the Su5 and tracer injection sites were histologically confirmed; the Su5 was an area in the supratrigeminal region at the level of the caudal two-thirds of the trigeminal motor nucleus (Mo5) and the level slightly caudal to the Mo5, and was positioned medially adjacent to the dorsomedial part of Pr5, as described previously (Fujio et.al 2016; see also introduction section). All of the injection sites covered some portion of the Su5 in eleven rats. Among these cases, the BDA injection sites were strictly confined to the Su5 in three rats. In a representative case, R810, the injection site was located in the center of the Su5 (Fig. 1C, D). We examined the distribution of anterogradely BDA-labeled axon fibers and terminals in and around the VPM (e.g., Fig. 2). In this case, the VPM was located between 2.30 mm and 4.52 mm cudal to bregma on the side contralateral to the BDA injection site. In the neighboring region, the

parvicellular part of ventral posterior thalamic nucleus (VPPC), the gustatory thalamus, was cytoarchitechtonically identified on the basis of well-known criteria described by Yasui et.al. (1989) and by Paxinos and Watson (1998) stereotaxic atlas. Many anterogradely BDA-labeled axon fibers and terminals were observed in the caudo-ventromedial edge of the VPM (termed VPMcvm) bilaterally with a contralateral predominance to the BDA injection site; the densest labeled terminals were seen at the level 4.16 mm caudal to bregma (Fig. 2C, E, F). Note that the VPMcvm could not be exactly distinguished from the remaining core part of VPM (termed core VPM: that is, the VPM excluding the VPMcvm) only on the basis of its cytoarchitecture (e.g. Figs. 2E, 3C). A small number of labeled fibers and terminals were seen in the VPPC bilaterally with a contralateral predominance. Labeled fibers and terminals were also observed scattered in the parafascicular nucleus and paracentral nucleus predominantly on the ipsilateral side. Importantly, no terminals were found in the core of VPM, posterior thalamic nucleus, submedial thalamic nucleus, or VPL.

Electrophysiological mapping of thalamic proprioceptive neurons

In the second experiment, we performed electrophysiological mapping of VPMcvm by recording the field potentials evoked by electrical stimulation of the masseter nerve and lingual nerve, and neuronal discharges to jaw-opening (e.g. Fig. 3) in three rats. During the mapping, these rats were immobilized with a neuromuscular junction blocker, and artificially ventilated, in order to minimize the influence of jaw-muscle contraction induced by electrical stimulation of each nerve. In a representative case, R909, large negative field potentials could be recorded only in the VPMcvm after masseter nerve stimulation; the exact locations of all recording sites were later confirmed histologically

(Fig. 3A-C). At the hotspot of VPMcvm (circled number 6 in Fig. 3B, C), the largest negative potentials with 4.0 msec latency were evoked by masseter nerve stimulation (circled number 6 in Fig. 3D). Multi-unit discharges that increased during passive, sustained jaw-opening movements were also recorded at this site (Fig. 3E). In the ventromedial part of the core VPM (circled number 3 in Fig. 3A, about 0.84 mm rostral to the site indicated by circled number 6), negative potentials with 4.2 ms latency were evoked by lingual nerve stimulation, whereas no responses were evoked by masseter nerve stimulation (circled number 3 in Fig. 3D).

Retrograde labeling of neurons projecting to VPMcvm

In the first experiment, it was demonstrated that there is a projection from the Su5 to the VPMcvm, but not to the core VPM. However, it remains unclear whether the VPMcvm receives projections from the Pr5 and Sp5. In the third experiment, aimed at addressing this issue, a retrograde tracer, WGA-HRP or FG, was injected into the VPMcvm in ten rats. In each rat, the VPMcvm was identified on the basis of electrophysiological recordings in the second experiment. Figure 4 shows the field potentials recorded in the VPMcvm in case R613, after the electrical stimulation of the masseter nerve (Fig. 4A), and multi-unit responses during passive, sustained jaw-opening movements (Fig. 4B). WGA-HRP was injected in six of the ten rats, and FG in other four rats. In all of the ten cases, the injection sites were histologically confirmed to cover at least a portion of the VPMcvm (e.g., Fig. 4C, D, F), and some neurons were retrogradely labeled in the Su5. The resultant distribution of the retrogradely labeled neurons is representatively shown in Table 1. In two of the ten cases (case R613 with a WGA-HRP injection and case R706 with an FG injection) in which injection sites were confined to the VPMcvm (e.g., Fig. 4C,

D), the retrogradely labeled neurons were seen only on the side contralateral to the injection site (e.g., Fig, 5). In case R613, for example, a large number of labeled neurons (n=159) were found throughout the Su5, especially in its caudal part (Fig. 5B-D, G). A considerable number of labeled neurons (n= 87) were also found in the dorsomedial edge of the Pr5 laterally adjacent to the Su5 (Fig. 5B- D, G). Only very few neurons were labeled in the intertrigeminal region (n= 5) (Fig. 5B-D, G), and in the area ventral to the Mo5 and medial to the Pr5 (n= 7) (Fig. 5C). On the other hand, we found no labeled neurons in any of the following structures: the parabrachial nucleus (Fig. 5A, B, F), remaining areas of the Pr5 (Fig. 5A-E, G) and Sp5 (Fig. 5E), the Mo5 (Fig. 5A-D, G) and the parvicellular reticular formation (Fig. 5A-E, G). In two other cases of the ten cases (R204, R211), the injection sites covered the VPMcvm, but extended into the VPPC medial to the VPMcvm (Fig. 4E). A small number of retrogradely labeled cells were also found bilaterally in the parabrachial nucleus dorsal or rostrodorsal to the Su5 (Table 1). In the remaining six cases of the ten cases, the injection sites covered the VPMcvm but extended into the core VPM lateral or rostrodorsal to the VPMcvm. The retrogradely labeled cells were also seen in the complex of the Pr5 and Sp5 (oral, interpolar and caudal parts): the injection site and the labeled neuron numbers in a representative case R100 are indicated in Fig. 4E and F, and Table 1, respectively.

Retrograde labeling of neurons projecting to core VPM

In the fourth experiment, we sought to compare the distribution patterns of neurons (including the Su5 neurons) projecting to the VPMcvm with those of Pr5/Sp5 projecting to the core VPM. Thus, we first injected a retrograde tracer in the core VPM of four rats at the site where the largest field potentials evoked by electrical stimulation of the lingual

nerve (Fig. 6A). In two cases (R115 with WGA-HRP injection and R225 with FG injection) out of the four cases, the injection site covered the ventromedial part of VPM rostral to the VPMcvm, but did not appear to extend into the VPMcvm (Figs. 4E, 6B, C). The distribution patterns of retrogradely neurons were different between the VPMcvm injection and the core VPM injection (Table 1). In case R115, for example, many labeled neurons (n= 236) were found in the Pr5 (except for its dorsomedial border) at the rostral level of Pr5 on the side contralateral to the injection site, whereas no neurons in the Su5 (Fig. 6D, E). Very few neurons (n= 2) were labeled in the intertrigeminal region, and no neurons were labeled in the area ventral to the Mo5 and medial to the Pr5, and the parabrachial nucleus. More caudally, a considerable number of labeled neurons (n= 34) were also seen in the Sp5, especially in the rostrodorsal region of the caudal part of the Sp5 (Fig. 6F).

In the second part of the fourth experiment, we injected a retrograde tracer in the core VPM where the largest field potentials were recorded after the electrical stimulation of the infraorbital nerve in two rats (case R219 with FG injection and case R310 with WGA-HRP injection). These injection sites were confirmed to the core VPM far from the VPMcvm (Fig. 4E, F). No neurons were labeled in the Su5 and dorsomedial edge of the Pr5, but many retrogradely FG-labeled neurons were widely distributed in the dorsoventrally middle two-thirds of Pr5 and Sp5, and especially in the caudal part of Sp5 (Table 1).

Discussion

The present study has for the first time revealed the detailed thalamic relay of JCMS sensory inputs; the relay site was confined to a small region in the VPM (i.e., VPMcvm) which had not been predicted in previous studies. This finding provides an important contribution to our understanding of the organization of ascending sensory proprioceptive pathways in the rat and could lead to new therapeutic approaches for the neurosurgical treatment of patients suffering from orofacial movement disorders.

Characteristics of experimental procedure

It has been generally recognized that forelimb and hindlimb proprioceptive information is conveyed to the rostrodorsal shell or rostral (oral) region (or VPLo) of VPL, and that these signals are relayed by neurons in the external cuneate nucleus and nucleus Z at least in rats, respectively (Low et al. 1987; Bolton and Tracey 1992). Jones and Friedman (1982) predicted that thalamic relay site of orofacial proprioception would be located in the rostrodorsal aspect of the VPM. However, their prediction is not consistent with our result: the thalamic relay site of orofacial proprioception was not in the "rostral" VPM, but in the "caudo-ventromedial" edge (VPMcvm) of VPM. The VPMcvm is a very small part of the VPM and thus would be difficult to delineate only by electrophysiological mapping of the very large VPM without the present morphological data which identify its position and extent. We should mention that our present results regarding the Su5-VPMcvm projection have been established based on previous findings (Fujio et al. 2016), which

precisely defined the location of rat Su5 and demonstrated that the rat Su5 neurons almost exclusively receive the JCMS inputs.

Characteristics of Su5 neurons projecting to VPMcvm

One of the main goals of our study was to examine the distribution patterns of neurons projecting to the electrophysiologically identified VPMcvm. The projection neurons to the VPMcvm were found not only in the Su5 but also in the dorsomedial edge of Pr5 laterally adjacent to the Su5 (Fig. 5B-D, G). Interestingly, Fujio et al. (2016) showed that both the Su5 and the dorsomedial edge of Pr5 laterally adjacent to the Su5 receive projections from the Me5 primary afferents innervating the JCMSs. These findings suggest that the neurons in the dorsomedial edge of Pr5 are functionally in the same class as the Su5 neurons, but not the same as the core Pr5 neurons.

It is known that the Me5 neurons conveying JCMS inputs centrally project not only to the Su5 but also to the dorsomedial region of the oral part of Sp5 and the parvicellular reticular formation, all of which contain premotoneurons projecting to the Mo5 (Luo et al. 2001). However, the present study has shown that the projection neurons to the VPMcvm are located only in the Su5, and not in the dorsomedial region of the oral part of Sp5 and parvicellular reticular formation. This difference strongly suggests that the Su5 neurons play an especially important role in the processing of proprioceptive signals and their relay to the thalamus, and, then, possibly to the cerebral cortex.

Parallel pathways to VPM

The first and second experiments of the present study have clearly shown that the JCMS inputs are conveyed by the Su5 neurons mainly to a very small area (VPMcvm) in the

VPM, but not to the core VPM (see summery diagram in Fig. 7). In the third experiment, in the cases where retrograde tracer injections were confined to the VPMcvm, labeled neurons were found only in the Su5, and none in the Pr5, Sp5 and parabrachial nucleus. In the cases where the injections were extended into the core VPM, the retrogradely labeled neurons were found not only in the Su5 but also in the Pr5 and Sp5. Collectively, these findings strongly suggest that the VPMcvm only receives the JCMS inputs via the Su5 neurons, and does not receive the orofacial inputs via the Pr5, Sp5 and parabrachial nucleus. In the fourth experiment, after retrograde tracers were injected into the lingual nerve area and infraorbital area of core VPM, labeled neurons were found mainly in the Pr5 and Sp5, and none in the Su5. These findings confirm the existence of projections from the Pr5 and Sp5 to the core of VPM, as shown elsewhere (Fukushima and Kerr 1979; Bruce et al. 1987; Kemplay and Webster 1989). Collectively, these findings have indicated the existence of two distinct trigeminothalamic pathways: the Su5-VPMcvm pathway and the Pr5/Sp5-core VPM pathway. Since the neurons in the Pr5 and Sp5 are known to receive primary afferent projections from trigeminal ganglion neurons (Marfurt 1981; Takemura et al. 1991), the present findings have further demonstrated that the Su5-VPMcvm pathway conveys only the JCMS inputs, while the Pr5/Sp5-coe VPM pathway conveys all of the other orofacial sensations including the other orofacial proprioceptive sensations.

Additionally, in the third experiment where the injection site covering the VPMcvm extended medially into the VPPC, retrogradely labeled neurons were found in the parabrachial nucleus as well as in the Su5. The VPPC (often called the gustatory

thalamus) is known to receive direct projections from the parabrachial nucleus (Norgren and Leonard 1973; Cechetto and Saper 1987; Krout and Loewy 2000) (Fig. 7).

The proprioceptive processing by the Pr5/Sp5-core VPM pathway was established by the following previous findings. The primary afferents innervating the tendons of masseter and temporal muscles arise from the trigeminal ganglion neurons in the cat (Cody et al. 1972; Lund et al. 1978). The nociceptive primary afferents innervating the fascia of masseter muscle also arise from the trigeminal ganglion neurons and project to the Pr5 and Sp5 in the rat (Dessem et al. 2007). The primary afferents innervating the capsule of the temporomandibular joint terminate in the Pr5 and Sp5 in cats (Romfh et al. 1979; Capra 1987). The core VPM of the rat receives the projections from the Sp5 secondary neurons that respond to the electrical stimulation of the capsule of the temporomandibular joint and the fascia of the masseter muscle (Ohya 1992; Ohya et al.1993). Collectively, these earlier findings support that the proprioceptive sensations arising from the JCMSs and from the other orofacial deep tissues (e.g., tendon, fascia and joint capsule) are transmitted by separate portions of the VPM (VPMcvm and core VPM).

Characteristics of Su5-VPMcvm pathway

The present study shows that Su5 neurons do not project to the posterior thalamic nucleus and submedial thalamic nucleus, although the neurons in the Pr5 and Sp5 are known to project to these thalamic nuclei in addition to the core VPM (Dado and Gieslern1990; Chiaia et al. 1991a, b; Fabri and Burton 1991; Yoshida et al. 1991; Diamond et al. 1992a, b; Veinante and Deschênes 1999; Pierret et al. 2000). It has been demonstrated that the posterior thalamic nucleus receives not only general somatic inputs but also auditory, visual and vestibular inputs and plays a role as the interface between sensory and motor

functions (Groenewegaen and Witter 2004), and that the submedial thalamic nucleus receives nociceptive inputs and projects to the prefrontal cortical area involved in autonomic and limbic functions (Dado and Giesler 1990; Yoshida et al. 1991, 1992). Therefore, the thalamic processing of JCMS inputs relayed through the Su5-VPMcvm pathway may have a specific but as yet unknown role, compared to that of the other orofacial sensory inputs (including the other proprioceptive inputs) conveyed through the Pr5 and Sp5.

Clinical application

The Vim in humans is considered to be homologous to the oral part (VPLo) of VPL in non-human primates. The Vim neurons respond to the passive and active movements of body parts and receive proprioceptive inputs (group Ia muscle spindle inputs) from the body. Lesions (thalamotomy) or DBS in the Vim have been effectively applied to parkinsonian and essential tremor patients to treat their tremor (Narabayashi and Ohye 1980; Ohye et al. 1989; Lenz et al. 1990, 1994; Ohye 2000; Hamani et al. 2006). On the other hand, in the present study, the "orofacial proprioceptive thalamus" VPMcvm which receives only JCMS inputs has for the first time been identified in rats. This finding suggests the existence of a similar region in other animals including humans. Thalamotomy or DBS in such a specific orofacial proprioceptive thalamic region corresponding to the rat VPMcvm might be an effective target for patients suffering from orofacial movement disorders, especially essential orofacial tremor (Clark et al.1993; Erer and Jankovic 2007; Wolraich et al. 2010; Karp and Alter 2016). Since the present study has demonstrated that the VPMcvm only receives JCMS inputs, targeting the "orofacial

proprioceptive thalamus" in human surgery might exert a curative effect on the patients without affecting other orofacial sensations.

References

Akhter F, Haque T, Sato F, Kato T, Ohara H, Fujio T, Tsutsumi K, Uchino K, Sessle BJ, Yoshida A (2014) Projections from the dorsal peduncular cortex to the trigeminal subnucleus caudalis (medullary dorsal horn) and other lower brainstem areas in rats. Neuroscience 266:23-37

Andersson SA, Landgren S, Wolsk D (1966) The thalamic relay and cortical projection of group I muscle afferents from the forelimb of the cat . J Physiol (Lond) 183:576-591

Bolton PS, Tracey DJ (1992) Neurons in the dorsal column nuclei of the rat respond to stimulation of neck mechanoceptors and project to the thalamus. Brain Res 595:175-179

Bruce LL, McHaffie JG, Stein BE (1987) The Organization of trigeminotectal and trigeminothalamic neurons in rodents: a double-labeling study with fluorescent dyes. J Comp Neurol 262:315-330

Capra NF (1987) Localization and central projections of primary afferent neurons that Innervate the temporomandibular joint in cats. Somatosens Res 4:201-213

Cechetto DF, Saper CB (1987) Evidence for a viscerotopic sensory representation in the cortex and thalamus in the rat. J Comp Neurol 262:27-45

Chiaia NL, Rhoades RW, Bennett-Clark CA, Fish SE, Killackey HP (1991a) Thalamic

processing of vibrissal information in the rat. I. Afferent input to the medial ventral posterior and posterior nuclei. J Comp Neurol 314:201-216

Chiaia NL, Rhoades RW, Fish SE, Killackey HP (1991b) Thalamic processing of vibrissal information in the rat: II. Morphological and functional properties of medial ventralposterior nucleus neurons. J Comp Neurol 314:217-236

Clark GT, Koyano K, Browne PA (1993) Oral motor disorders in humans. J Calif Dent Assoc 21:19-30

Cody FW, Lee RW, Taylor A (1972) A functional analysis of the components of the mesencephalic nucleus of the fifth nerve in the cat. J Physiol (Lond) 226:249-261

Dado RJ, Giesler Gr Jr (1990) Afferent input to nucleus submedius in rats: retrograde labeling of neurons in the spinal cord and caudal medulla. J Neuroscience 10:2672-2686

Dessem D, Moritani M, Ambalavanar R (2007) Nociceptive craniofacial muscle primary afferent neurons synapse in both the rostral and caudal brain stem. J Neurophysiol 98:214-223

Diamond ME, Armstrong-James M, Budway MJ, Ebner FF (1992a) Somatic sensory responses in the rostral sector of the posterior group (POm) and in the ventral posterior medial nucleus (VPM) of the rat thalamus: dependence on the barrel field cortex. J Comp Neurol 319:66-84

Diamond ME, Armstrong-James M, Ebner FF (1992b) Somatic sensory responses in the

rostral sector of the posterior group (POm) and in the ventral posterior medial nucleus (VPM) of the rat thalamus. J Comp Neurol 318:462-476

Dubner R, Sessle BJ, Storey AT (1978) The neural basis of oral and facial function. New York: Plenum Press

Erer S, Jankovic J (2007) Hereditary chin tremor in Parkinson's disease. Clin Neurol Neurosurg 109:784-785

Fabri M, Burton H (1991) Topography of connections between primary somatosensory cortex and posterior complex in rat: a multiple fluorescent tracer study. Brain Res 538:351-357

Francis JT, Xu S, Chapin JK (2008) Proprioceptive and cutaneous representations in the rat ventral posterolateral thalamus. J Neurophysiol 99:2291-2304

Friedman DP, Jones EG (1981) Thalamic input to areas 3a and 2 in monkeys. J Neurophysiol 45:59-85

Fujio T, Sato F, Tachibana Y, Kato T, Tomita A, Higashiyama K, Ono T, Maeda Y, Yoshida A (2016) Revisiting the supratrigeminal nucleus in the rat. Neuroscience 324:307-320

Fukushima T, Kerr FW (1979) Organization of trigeminothalamic tracts and other thalamic afferent systems of the brainstem in the rat: presence of gelatinosa neurons with thalamic connections. J Comp Neurol 183:169-184

Groenewegen HJ, Witter MP (2004) Thalmus. In Paxinos G, editor. nervous

system.Amsterdam: ElsevierAcademic Press. pp 407-453

Hamani C, Dostrovsky JO, Lozano AM (2006) The motor thalamus in neurosurgery. Neurosurgery 58:146-158

Jones EG, Friedman DP (1982) Projection pattern of functional components of thalamic ventrobasal complex on monkey somatosensory cortex. J Nurophysiol 48:521-544

Jones EG, Friedman DP, Hendry SH (1982) Thalamic basis of place- and modality-specific Columns in Monkey somatosensory cortex: a correlative anatomical and physiological study. J Neurophysiol 48:545-568

Karp BI, Alter K (2016) Botulinum toxin treatment of blepharospasm, orofacial/oromandibular dystonia and hemifacial spasm. Semin Neurol 36:84-91

Kemplay S, Webster KE (1989) A quantative study of the projections of the gracile, cuneate and trigeminal nucleiand of the medullary reticular formation to the thalamus in the rat. Neuroscience 32:153-167

Krout KE, Loewy AD (2000) Parabrachial nucleus projections to midline and intralaminar thalamic nuclei of the rat. J Comp Neurol 428:475-494

Lenz FA, Kwan HC, Dostrovsky JO, Tasker RR, Murphy JT, Lenz YE (1990) Single unit analysis of the human ventral thalamic nuclear group. Activity correlated with movement. Brain 113:1795-1821

Lenz FA, Kwan HC, Martin R, Tasker R, Richardson RT, Dostrovsky JO (1994) Charactersticks of somatotopic organization and spontaneous neural activity in the

region of the thalamic principal sensory nucleus in patients with spinal cord transection. J Neurophysiol 72:1570-1587

Leong SK, Tan CK (1987) Central projection of rat sciatic nerve fibers as revealed by Ricinus communis agglutinin and horseradish peroxidase tracers. J Anat 154:15-26

Lorente de Nó R (1922) Contribución a1 conocimiento del nerviotrigémino. Libro en. honor de Dn. S. Ramón y Cajal. Móya, Madrid, 2:13

Lorente de Nó R (1933) Vestibulo-ocular reflex arc. Arch Neurol Psychiatr 30:245–291

Low JS, Mantle-St John LA, Tracey DJ (1986) Nucleus z in the rat: spinal afferents from collaterals of dorsal spinocerebellar tract neurons. J Comp Neurol 243:510–526

Lund JP, Richmond FJ, Touloumis C, Patry Y, Lamarre Y (1978) The distribution of Golgi tendon organs and muscle spindles in masseter and temporalis muscles of the cat. Neuroscience 3:259–270

Luo P, Dessem D (1995) Inputs from identified jaw-muscle spindle afferents to trigeminothalamic neurons in the rat: a double-labeling study using retrograde HRP and intracellular biotinamide. J Comp Neurol 353:50–66

Luo P, Wong R, Dessem D (1995) Ultrastructural basis for synaptic transmission between jaw- muscle spindle afferents and trigeminothalamic neurons in the rostral trigeminal sensory nuclei of the rat. J Comp Neurol 363:109–128

Luo P, Moritani M, Dessem D (2001) Jaw-muscle spindle afferent pathways to the trigeminal motor nucleus in the rat. J Comp Neurol 435:341–353

Maendly R, Rüegg DG, Wiesendanger M, Wiesendanger R, Lagowska J, Hess B (1981) Thalamic relay for group I muscle afferents of forelimb nerves in the monkey. J Neurophysiol 46:901– 917

Marfurt CF (1981) The central projections of trigeminal primary afferent neurons in the cat as determined by the tranganglionic transport of horseradish peroxidase. J Comp Neurol 203:785– 798

Mesulam MM (1978) Tetramethyl benzidine for horseradish peroxidase neurohistochemistry: a non-carcinogenic blue reaction product with superior sensitivity for visualizing neural afferents and efferents. J Histochem Cytochem 126:106–117

Narabayashi H, Ohye C (1980) Importance of microstereoencephalotomy for tremor alleviation. Appl Neurophysiol 43:222–227

Norgren R, Leonard CM (1973) Ascending central gustatory pathways. J Comp Neurol 150:217–237

Ohya A (1992) Responses of trigeminal subnucleus interpolaris neurons to afferent inputs from deep oral structures. Brain Res Bull 29:773–781

Ohya A, Tsuruoka M, Imai E, Fukunaga H, Shinya A, Furuya R, Kawawa T, Matsui Y (1993) Thalamic- and cerebellar-projecting interpolaris neuron responses to afferent inputs. Brain Res Bull 32:615–621

Ohye C (2000) Use of selective thalamotomy for various kinds of movement disorder,

based on basic studies. Stereotact Funct Neurosurg 75:54–65

Ohye C, Shibazaki T, Hirai T, Wada H, Hirato M, Kawashima Y (1989) Further physiological observations on the ventralis intermedius neurons in the human thalamus. J Neurophysiol 61:488–500

Paxinos G, Watson C (1998) The rat brain in stereotaxic coordinates, 4th edn. Academic Press, Sydney

Paxinos G, Watson C (2007) The rat brain in stereotaxic coordinates, 6th edn. Academic Press, Sydney

Paxinos G, Watson C (2014) The rat brain in stereotaxic coordinates, 7th edn. Academic Press, Sydney

Pierret T, Lavallée P, Deschênes M (2000) Parallel streams for the relay of vibrissal information through thalamic barreloids. J Neurosci 20:7455–7462

Romfh JH, Capra NF, Gatipon GB (1979) Trigeminal nerve and temporomandibular joint of the cat: a horseradish peroxidase study. Exp Neurol 65:99–106

Sato F, Akhter F, Haque T, Kato T, Takeda R, Nagase Y, Sessle BJ, Yoshida A (2013) Projections from the insular cortex to painreceptive trigeminal caudal subnucleus (medullary dorsal horn) and other lower brainstem areas in rats. Neuroscience 233:9–27

Shigenaga Y, Nakatani Z, Nishimori T, Suemune S, Kuroda R, Matano S (1983) The cells of origin of cat trigeminothalamic projections: especially in the caudal medulla.

Brain Res 277:201–222

Takemura M, Sugimoto T, Shigenaga Y (1991) Difference in central projection of primary afferents innervating facial and intraoral structures in the rat. Exp Neurol 111:324–331

Taylor A (1990) Neurophysiology of the jaws and teeth. Macmillan Press, London

Veinante P, Deschênes M (1999) Single- and multi-whisker channels in the ascending projections from the principal trigeminal nucleus in the rat. J Neurosci 19:5085–5095

Wolraich D, Vasile Marchis-Crisan C, Redding N, Khella SL, Mirza N (2010) Laryngeal tremor: co-occurrence with other movement disorders. ORL J Otorhinolaryngol Relat Spec 72:291–294

Yasui Y, Saper CB, Cechetto DF (1989) Calcitonin gene-related peptide immunoreactivity in the visceral sensory cortex, thalamus, and related pathways in the rat. J Comp Neurol 290:487–501

Yoshida A, Dostrovsky JO, Sessle BJ, Chiang CY (1991) Trigeminal projections to the nucleus submedius of the thalamus in the rat. J Comp Neurol 307:609–625

Yoshida A, Dostrovsky JO, Chiang CY (1992) The afferent and efferent connections of the nucleus submedius in the rat. J Comp Neurol 324:115–133

Yoshida A, Taki I, Chang Z, Iida C, Haque T, Tomita A, Seki S, Yamamoto S, Masuda Y, Moritani M, Shigenaga Y (2009) Corticofugal projections to trigeminal motoneurons

innervating antagonistic jaw muscles in rats as demonstrated by anterograde and retrograde tract tracing. J Comp Neurol 514:368–386

Figure legends

Fig. 1

Field potential recorded in the supratrigeminal nucleus (Su5) (A, B) and location of a tracer injection site into the recording site (C, D) in case R810. A: Field potential in response to electrical stimulation of the masseter nerve. B: Extracellular multi-unit discharges recorded during a sustained jaw-opening movement (for about 5 s indicated by the horizontal bar). C, D: Reconstruction showing location of injection site (a field area) of the anterograde tracer, biotinylated dextranamine (BDA) in the Su5 360 μm rostral to the caudal end of the trigeminal motor nucleus (Mo5). The blue boxed area in C indicates the area shown in D. The section D is counterstained with Neutral red, and the injection site is revealed by the dark brown patch. For abbreviations see list.

Fig. 2

Distribution of anterogradely labeled axon terminals (red small dots) in the dorsal thalamus after a BDA injection in the Su5 in case R810. The injection site is presented in Fig. 1C, D. Coronal sections are arranged rostrocaudally from A to D. Numbers denote distance in millimeters caudal (–) to bregma on the contralateral (contra) side to the injection site. Note that the largest number of BDA-labeled terminals was seen, at the level 4.16 mm caudal to bregma, in the caudo-ventromedial edge (VPMcvm) of the ventral posteromedial thalamic nucleus (VPM) contralateral to the BDA injection site. In this case, the VPM was located at the levels from 2.30 to 4.52 mm caudal to bregma on the contralateral side. The boxed area in C indicates the area shown in E. E, F:

Photomicrographs showing BDA-labeled axon fibers and terminals in the contralateral VPMcvm. Area boxed in E corresponds to the area in F. Sections E, F are counterstained with Neutral red. For abbreviations see list.

Fig. 3

Drawings (A, B) and a photomicrograph (C) showing recording sites, and field potentials recorded in and around the VPMcvm (D, E) in case R909. A, B: Sections showing the contralateral side to the stimulated nerve are arranged rostrocaudally. Numbers denote distance in millimeters caudal (-) to bregma. A–C: Thick, black vertical lines indicate bleeding caused by microelectrode penetration. A, B: Each electrode penetration track is indicated by a red vertical line and is reconstructed on the basis of microdrive readings and visible electrode tracks observed in the sections. Short red, transverse bars indicate recording sites. Each small, blue boxed area, which is presented in the core VPM (A) or VPMcvm (B), indicates an area shown in the larger, blue boxed inset at lower left. B, C: The area bracketed with dashed green lines in B indicates the area shown in C. D: Field potentials evoked by masseter nerve stimulation and lingual nerve stimulation are presented in the left and right columns, respectively. In this case, the animal was paralyzed with a neuromuscular junction blocker. Field potentials indicated by circled numbers were recorded at the site indicated by the same circled numbers shown in the insets of A or B. Field potentials indicated by circled number 9 were recorded at the site just caudal to the site indicated by circled number 6. An arrow and an arrowhead in D indicate 4.2 and 4.0 ms latency, respectively. E: Extracellular multi-unit discharges recorded at the site indicated by circled number 6 during a sustained jaw-opening movement (for about 2.3 s indicated by a horizontal line). For abbreviations see list.

Fig. 4

Field potential recorded in the VPMcvm (A, B) and locations of tracer injection sites (C–F). The examples shown in A–D were obtained in case R613. A: Field potential evoked by electrical stimulation of the masseter nerve contralateral to the recording site. Note that, in this case, the animal was not paralyzed with a neuromuscular junction blocker. B: Extracellular multi-unit discharges recorded during a sustained jaw-opening movement (for about 3.7 s indicated by a horizontal line). C, D: A drawing and a photomicrograph showing the injection site of wheat-germ agglutinin conjugated horseradish peroxidase (WGA-HRP) (a filled area in C) made at the recording site. The injection center was found in the VPMcvm contralateral to the stimulated masseter nerve in a coronal section 4.16 mm caudal (–) to bregma. The blue boxed area in C indicates the region shown in D. The section D was reacted with diaminobenzidine (DAB) and weakly counterstained with Neutral red. E, F: Semi-schematic drawings of the location of injection sites in the coronal section 3.30 and 4.16 mm caudal (–) to bregma in nine cases (including case R613 shown in C). The injection site in case R115 is also shown in Fig. 6B. Injection sites in cases R310 and R100 are present in both of the sections since they extended rostrocaudaly to both levels. Note that WGA-HRP and FG were injected in cases R613, R204, R211, R115 and R310 and cases R706, R100, R225 and R219, respectively (also see Table 1). For abbreviations see list.

Fig. 5

Distribution of retrogradely labeled neurons (dots) in the pons after WGA-HRP injection in the VPMcvm in case R613. The injection site is presented in Fig. 4C, D. Coronal sections contralateral to the injection site are arranged rostrocaudally from A to E.

Numbers denote distance in micrometers rostral and caudal (–) to the caudal end of Mo5. In this case, the rostral end of Su5 was located 720 μm rostral to the caudal end of Mo5. The blue boxed area in A and green boxed area in C indicate areas shown in F and G, respectively. F, G: Dark field photomicrographs of non-counterstained sections.

Fig. 6

Field potential evoked in the core VPM (A) and WGA-HRP injection site made at the recording site (B, C), and the resultant distribution of retrogradely WGA-HRP labeled neurons (D–F) in case R115. A: The average field potential evoked by electrical stimulation of the lingual nerve, which was recorded in the core part of VPM contralateral to the lingual nerve. B: The recording site in the core VPM just rostral to the VPMcvm (at the level 3.30 mm caudal to bregma), where WGA-HRP was subsequently injected (its injection site is denoted by a filled area). The injection site is also shown in Fig. 4E. The blue boxed area in B indicates the area shown in C. The section in C was reacted with DAB and counterstained with Neutral red. D: Retrogradely labeled neurons (dots) in the dorsomedial part of the principal sensory trigeminal nucleus (Pr5) at the level 450 μm rostral to the caudal end of Mo5 on the side contralateral to the injection site. The green boxed area in D indicates the area shown in E (dark field photomicrograph of non-counterstained section). F: Retrogradely labeled neurons (dots) in the rostral region of the caudal part of spinal trigeminal nucleus (630 μm rostral to the obex) on the side contralateral to the injection site. For abbreviations see list.

Fig. 7

Summary diagram showing the ascending thalamic projection (red) from the Su5 to the VPMcvm in comparison with those (blue) from the Pr5 (and spinal trigeminal nucleus) and parabrachial nucleus (PB), which have previously been described (for references, see text). Note that the diagram shows only the contralateral thalamic projections. However, in fact, the PB projection to the parvicellular part of ventral posterior thalamic nucleus (VPPC) is bilateral. For abbreviations see list.

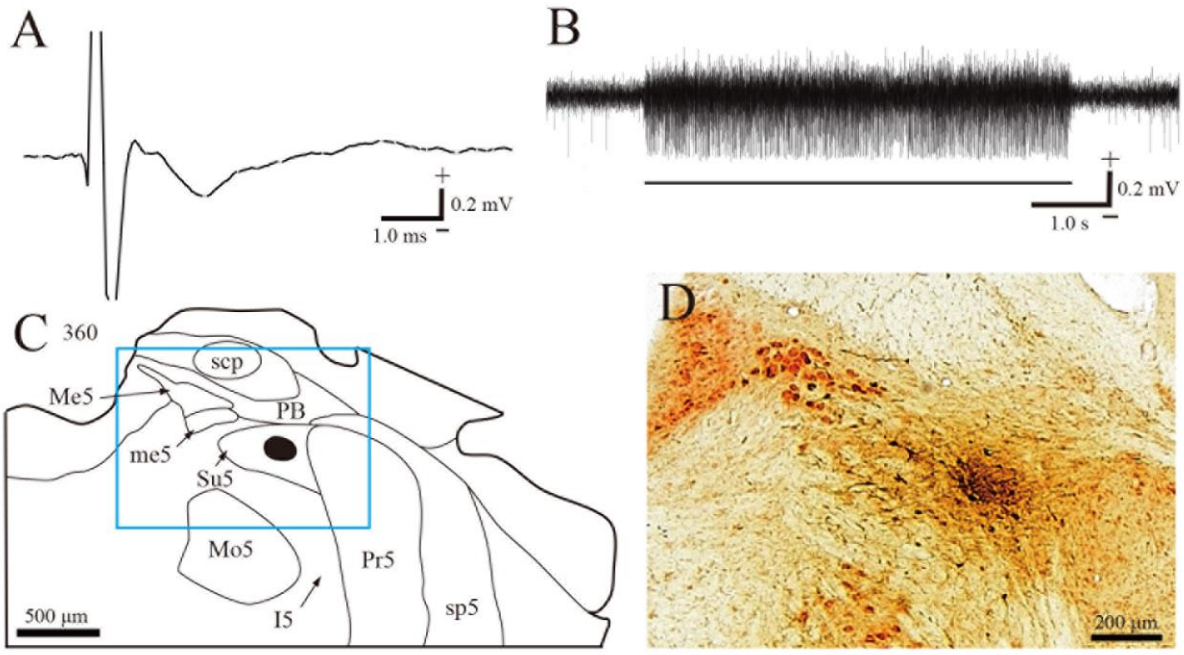
A
0.2 mV
1.0 ms
B
0.2 mV
1.0 s
C
360
scp
Me5
PB
me5
Su5
Mo5
Pr5
sp5
I5
500 µm
D
200 µm

Fig. 1

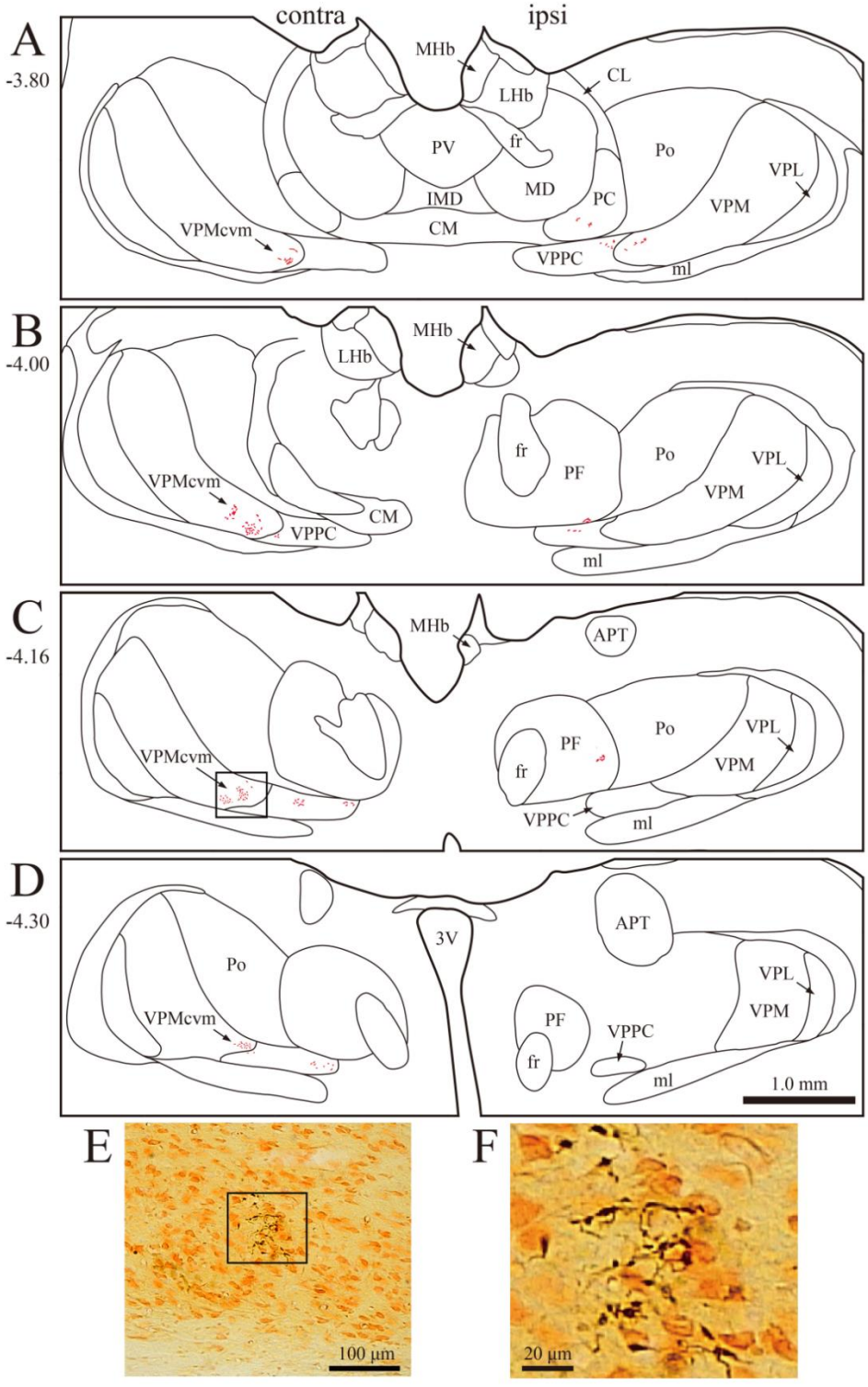
A
-3.80
contra
ipsi
MHb
LHb
CL
PV
fr
Po
VPL
IMD
MD
PC
VPM
CM
VPMcvm
VPPC
ml
B
-4.00
MHb
LHb
fr
PF
Po
VPL
VPM
VPMcvm
CM
VPPC
ml
C
-4.16
MHb
APT
PF
Po
VPL
VPM
VPMcvm
fr
VPPC
ml
D
-4.30
3V
APT
Po
VPL
VPM
VPMcvm
PF
VPPC
fr
ml
1.0 mm
E
100 µm
F
20 µm

Fig. 2

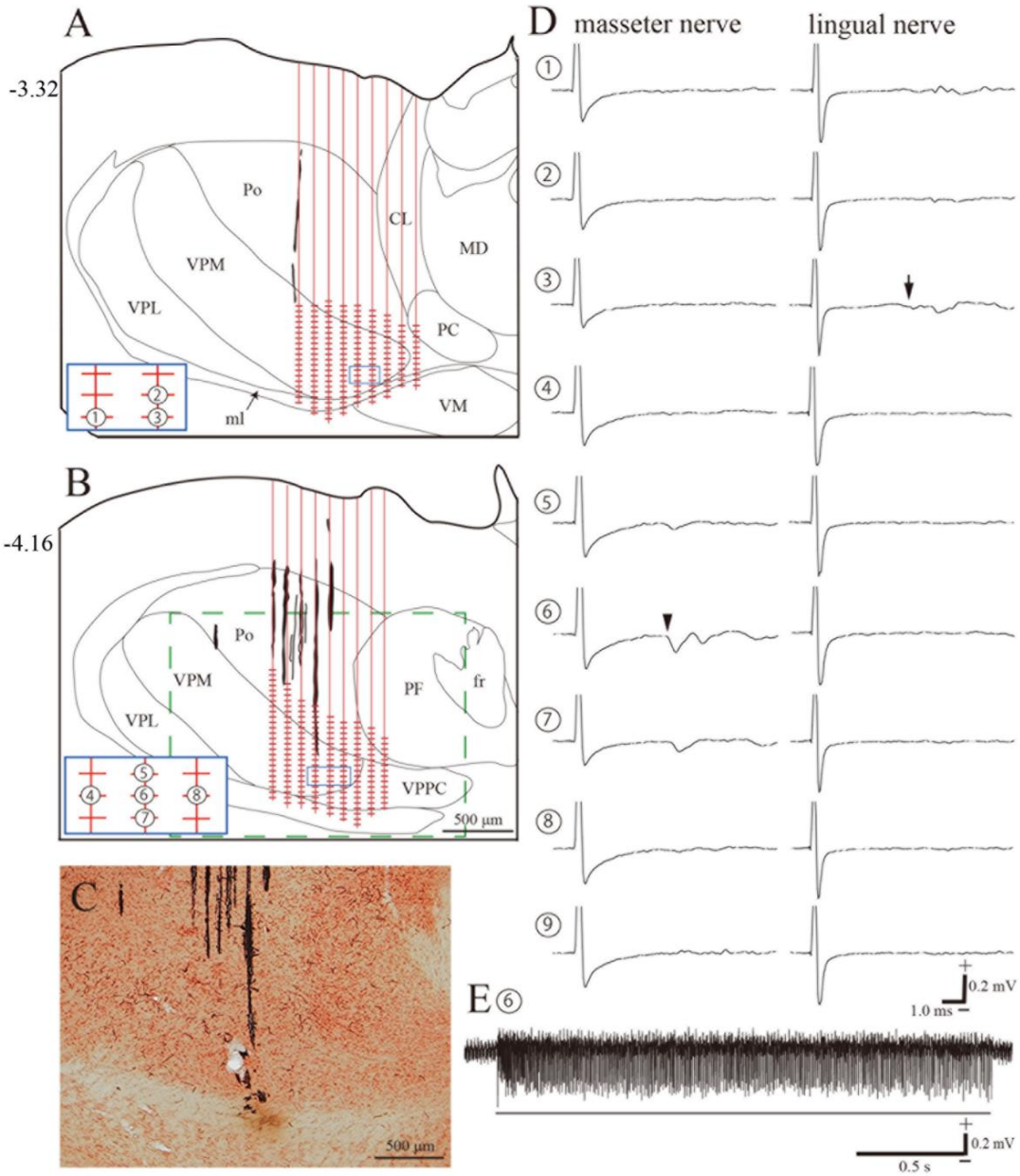
A
-3.32
Po
CL
MD
VPM
VPL
PC
VM
ml
B
-4.16
Po
VPM
VPL
PF
fr
VPPC
500 μm
C
500 μm
D
masseter nerve
lingual nerve
E
0.2 mV
1.0 ms
0.2 mV
0.5 s

Fig. 3

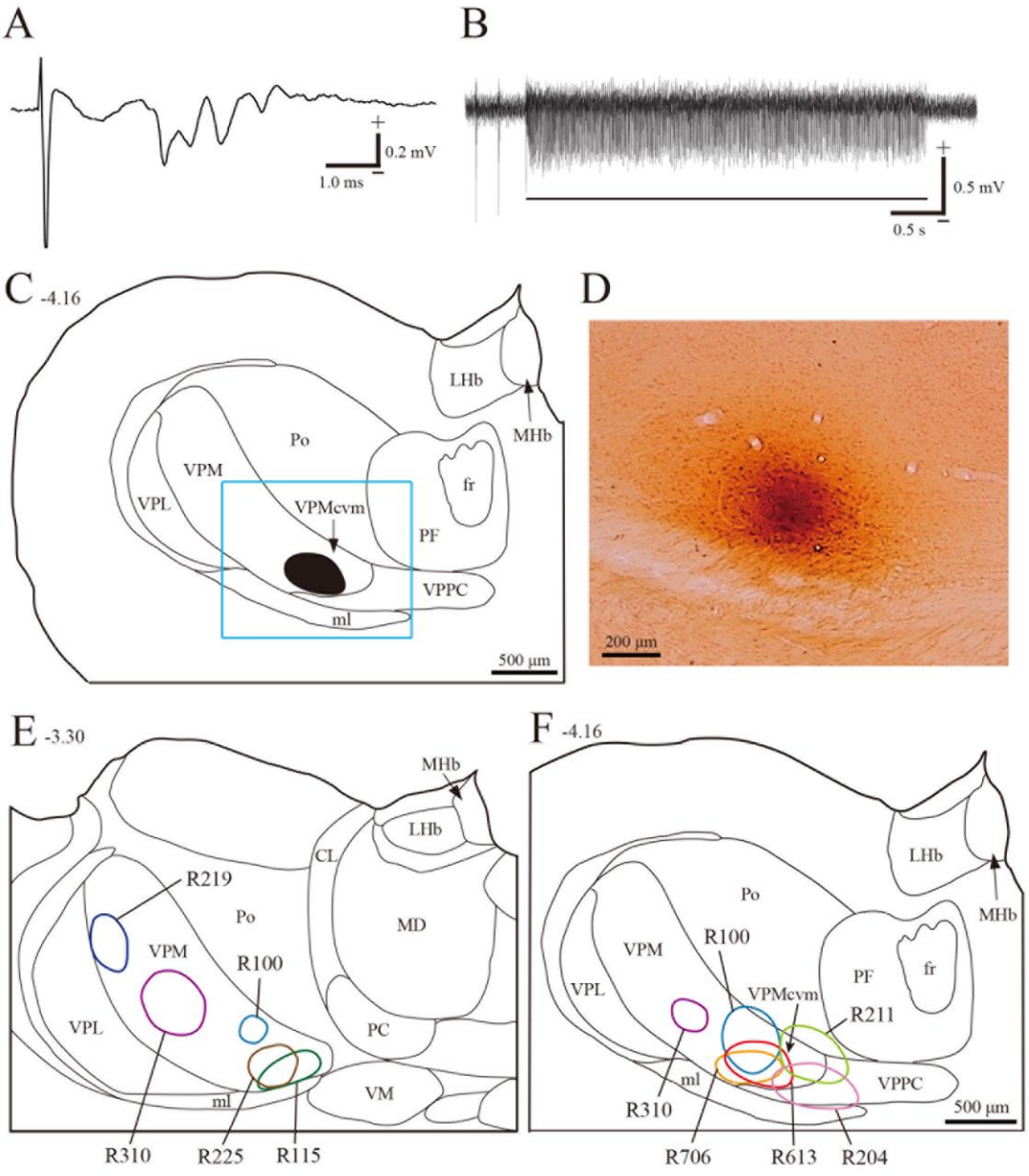
A
0.2 mV
1.0 ms
B
0.5 mV
0.5 s
C -4.16
LHb
MHb
Po
VPM
VPL
VPMcvm
fr
PF
VPPC
ml
500 µm
D
200 µm
E -3.30
MHb
LHb
CL
R219
Po
MD
VPM
R100
VPL
PC
VM
ml
R310
R225
R115
F -4.16
LHb
MHb
Po
VPM
R100
VPL
VPMcvm
PF
fr
R211
ml
VPPC
R310
500 µm
R706
R613
R204

Fig. 4

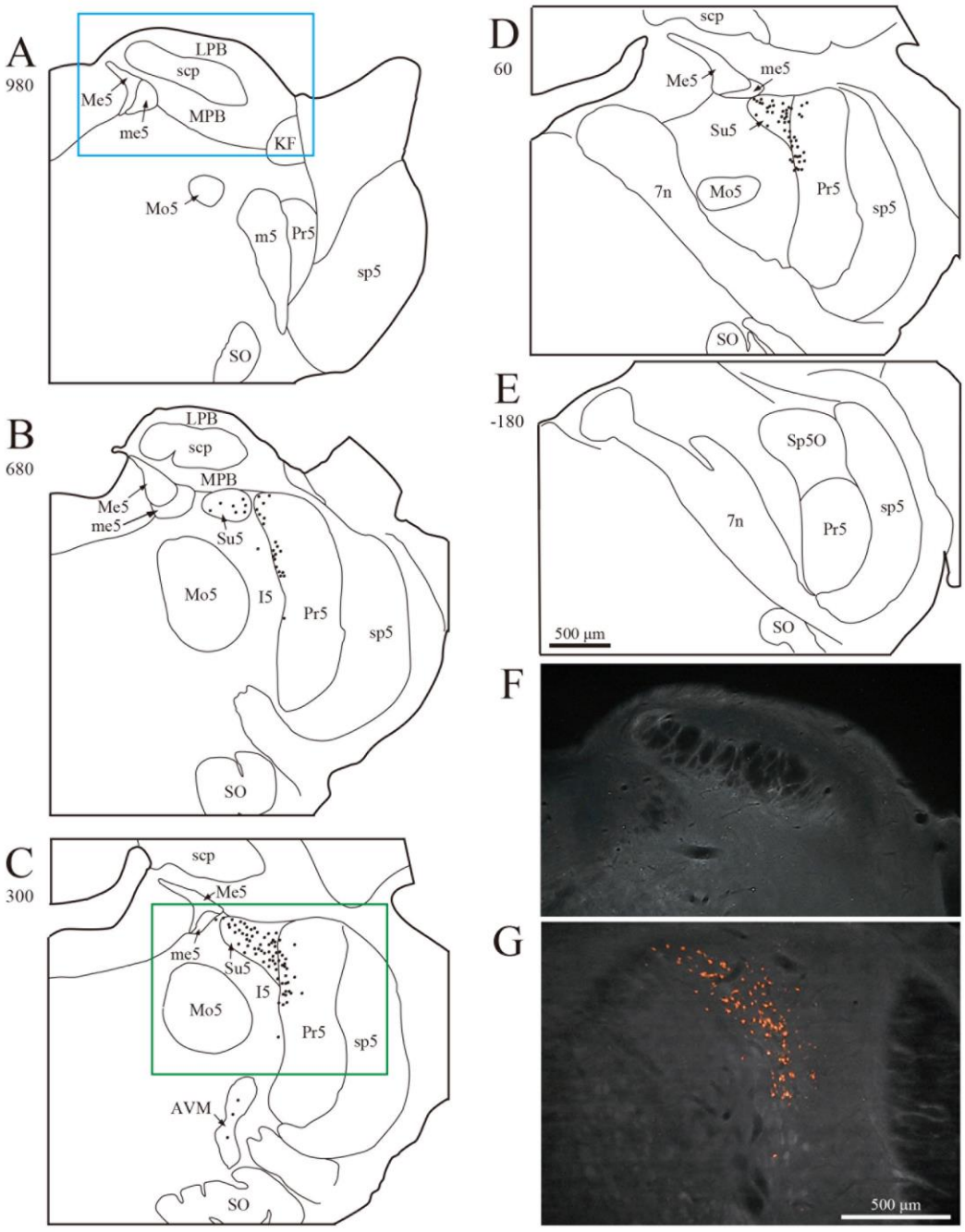
A
980
LPB
scp
Me5
me5
MPB
KF
Mo5
m5
Pr5
sp5
SO
B
680
LPB
scp
MPB
Me5
me5
Su5
Mo5
I5
Pr5
sp5
SO
C
300
scp
Me5
me5
Su5
I5
Mo5
Pr5
sp5
AVM
SO
D
60
scp
Me5
me5
Su5
7n
Mo5
Pr5
sp5
SO
E
-180
Sp5O
7n
Pr5
sp5
500 µm
SO
F
G
500 µm

Fig. 5

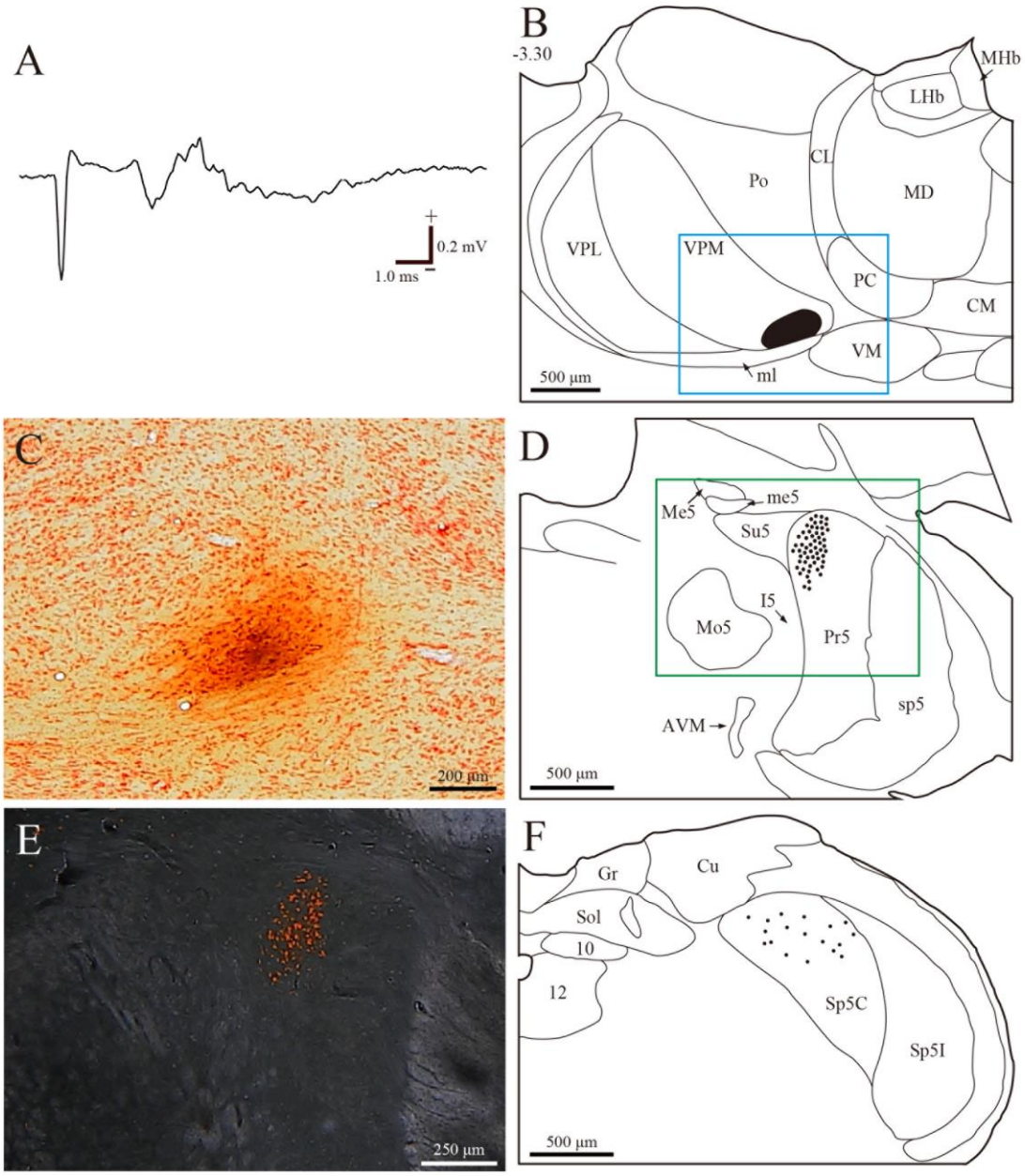
A
0.2 mV
1.0 ms
B
-3.30
MHb
LHb
CL
Po
MD
VPL
VPM
PC
CM
VM
ml
500 µm
C
200 µm
D
Me5
me5
Su5
I5
Mo5
Pr5
sp5
AVM
500 µm
E
250 µm
F
Gr
Cu
Sol
10
12
Sp5C
Sp5I
500 µm

Fig. 6

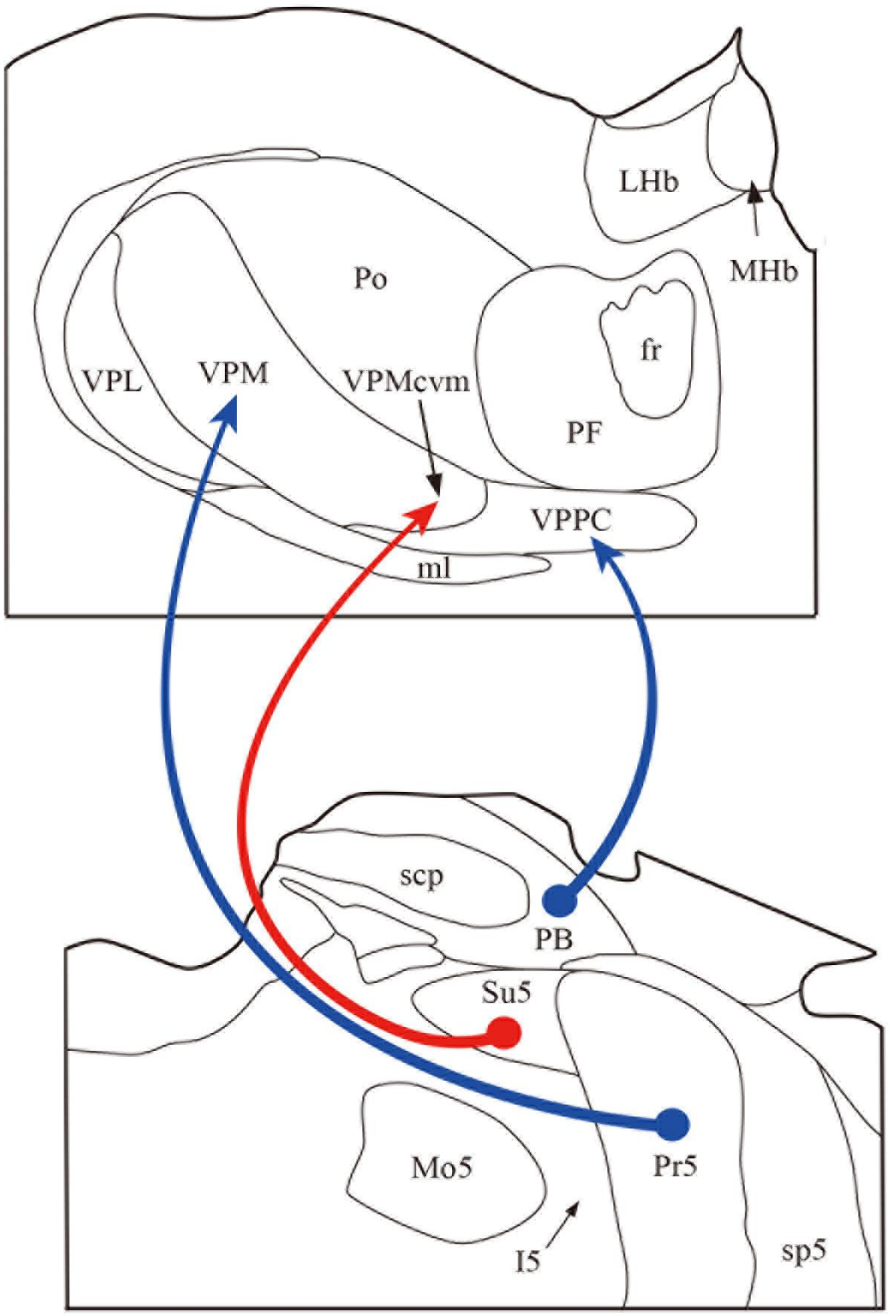

Fig. 7

Table 1. Distribution of retrogradely labeled neurons after tracer injections in and around VPM

Main injection site	Case No.	Tracer	Contralateral							Ipsilateral
			Su5	Dorsomedial edge of Pr5	Pr5	Sp5	I5	AVM	PB	PB
3rd experiment										
VPMcvm	R613	WGA-HRP	159	87	0	0	5	7	0	0
VPMcvm	R706	FG	76	60	0	9	3	0	0	0
VPMcvm + VPPC	R204	WGA-HRP	41	53	0	0	3	0	21	18
VPMcvm + VPPC	R211	WGA-HRP	30	60	0	0	6	14	18	27
VPMcvm + core VPM	R100	FG	38	95	161	42	11	14	0	0
4th experiment										
Core (lingual) VPM	R115	WGA-HRP	0	20	236	34	2	0	0	0
Core (lingual) VPM	R225	FG	0	10	118	19	1	0	0	0
Core (infraorbital) VPM	R219	FG	0	0	259	97	0	4	0	0
Core (infraorbital) VPM	R310	WGA-HRP	0	0	145	55	0	15	0	0

Numbers of retrogradely labeled neurons were counted in every third section. For abbreviations see list.